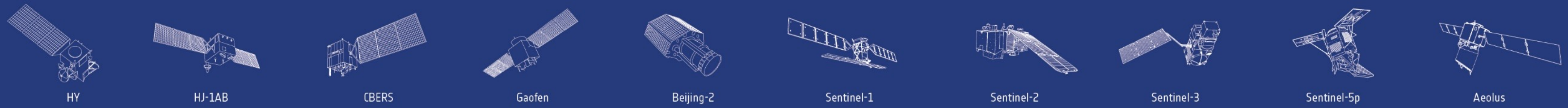

2023 DRAGON 5 SYMPOSIUM

3rd YEAR RESULTS REPORTING

11-15 SEPTEMBER 2023

[PROJECT ID. 58817]

[UAVS 4 HIGH-RES. OPTICAL SATS.]

REPORTING TIME: WEDNESDAY 13/09/2023

ID. 58817

PROJECT TITLE: Exploiting UAVs for validating decametric earth observation data from Sentinel-2 and Gaofen-6(UAV4VAL)

PRINCIPAL INVESTIGATORS: Yongjun Zhang, Jadunandan Dash, Yan Gong, Hu Tang, Xuerui Guo

CO-AUTHORS: Harry Morris, Gareth Roberts, Booker Ogutu, Shenghui Fang, Niall Origo

PRESENTED BY: Yan Gong

Dragon 5 3rd Year Results Reporting

- Inform on the project's objectives
- Detail the Copernicus Sentinels, ESA, Chinese and ESA Third Party Mission data utilised after 3 years
- Detail the in-situ data measurements and requirements
- Provide details on field data collection campaigns and periods in P.R. China or other study areas
- Inform on the results after 3 years of activity
- Inform on the project's schedule, planning & contribution of the partners for the following year
- Report on the level and training of young scientists on the project achievements, including plans for academic exchanges
- Report on the peer reviewed publications (nr. of papers, journal name and publication title) after 3 years of activity

Background

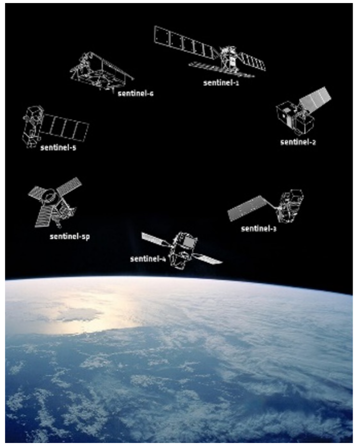

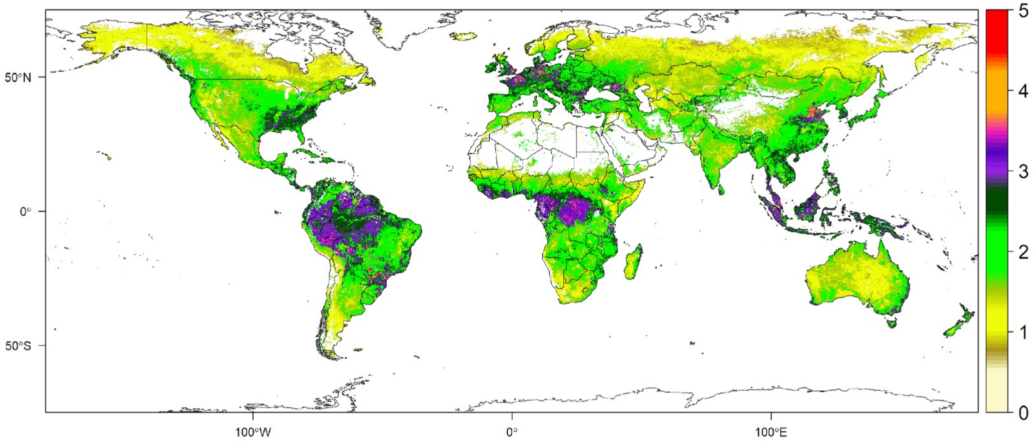

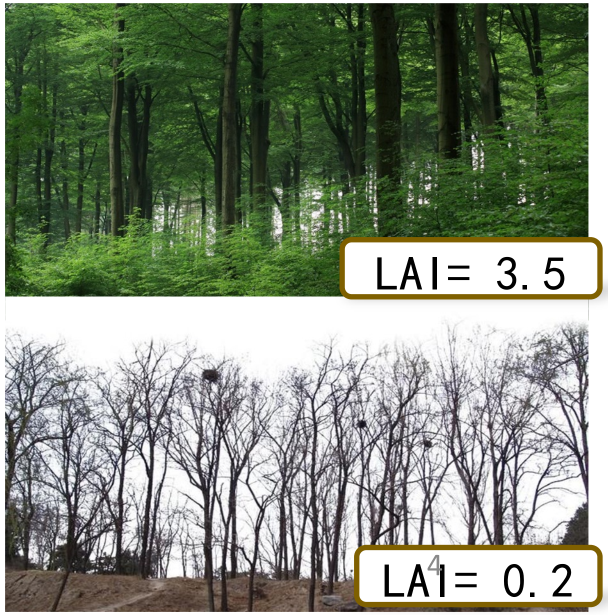

- **Vegetation biophysical variables such as Leaf Area Index (LAI), Canopy Chlorophyll content (CCC), Fraction of absorbed Photosynthetic Radiation (fAPAR) are important plant and ecosystem status indicators.**
- **Advances in sensing and retrieval techniques -> suitability in operational use**
- **Validation is crucial to ensure fit-for-purpose**
- **Field campaigns are logistically challenging and resource intensive**
- **Automated measurement the way forward**
- **UAV Remote Sensing multi images Radiation Calibration**

The project’s objectives: UAV4VAL

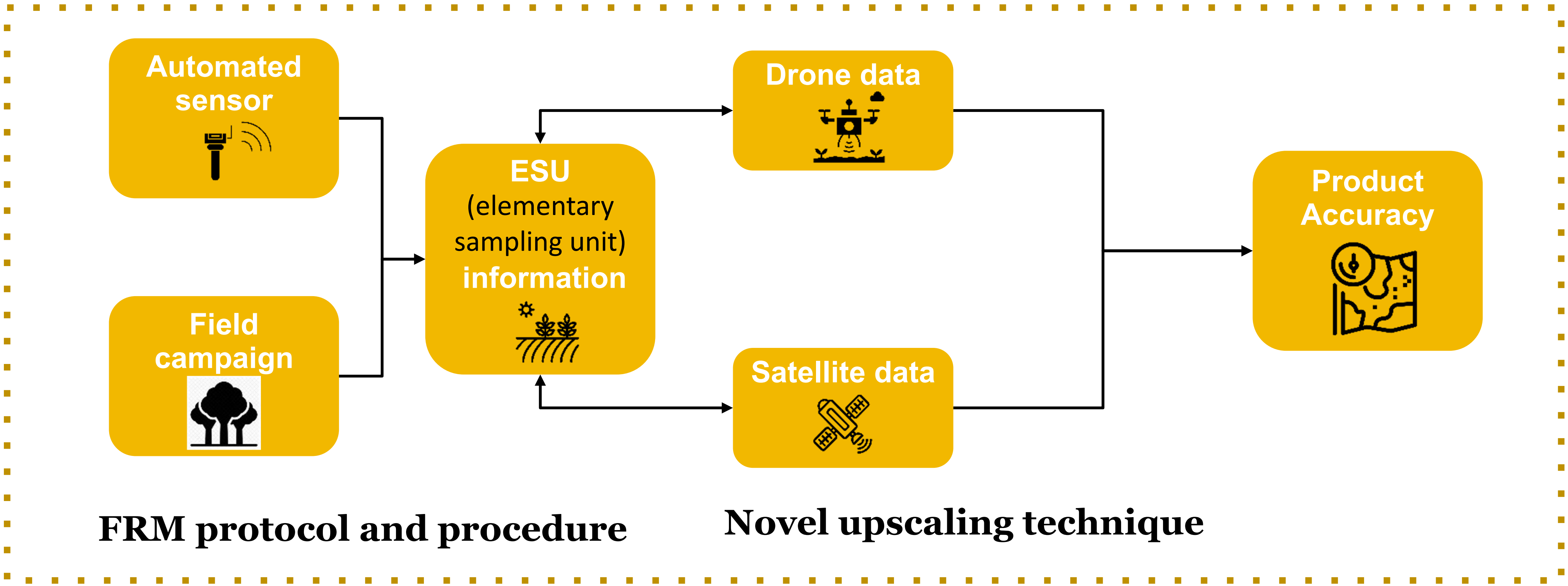

The project’s objectives: UAV4VAL

- **Evaluate the capability of UAVs as a source of reference data for validating decametric surface reflectance and vegetation products, (specific focus on Sentinel-2 and Gaofen-6)**

- **Transfer knowledge gained from existing ESA-funded projects on fiducial reference measurements (FRM), which focus on traceability and uncertainty evaluation in earth observation validation efforts**

- **Achieved through collection, processing, and analysis of ground measurements over European and Chinese sites, coinciding with UAV acquisitions**

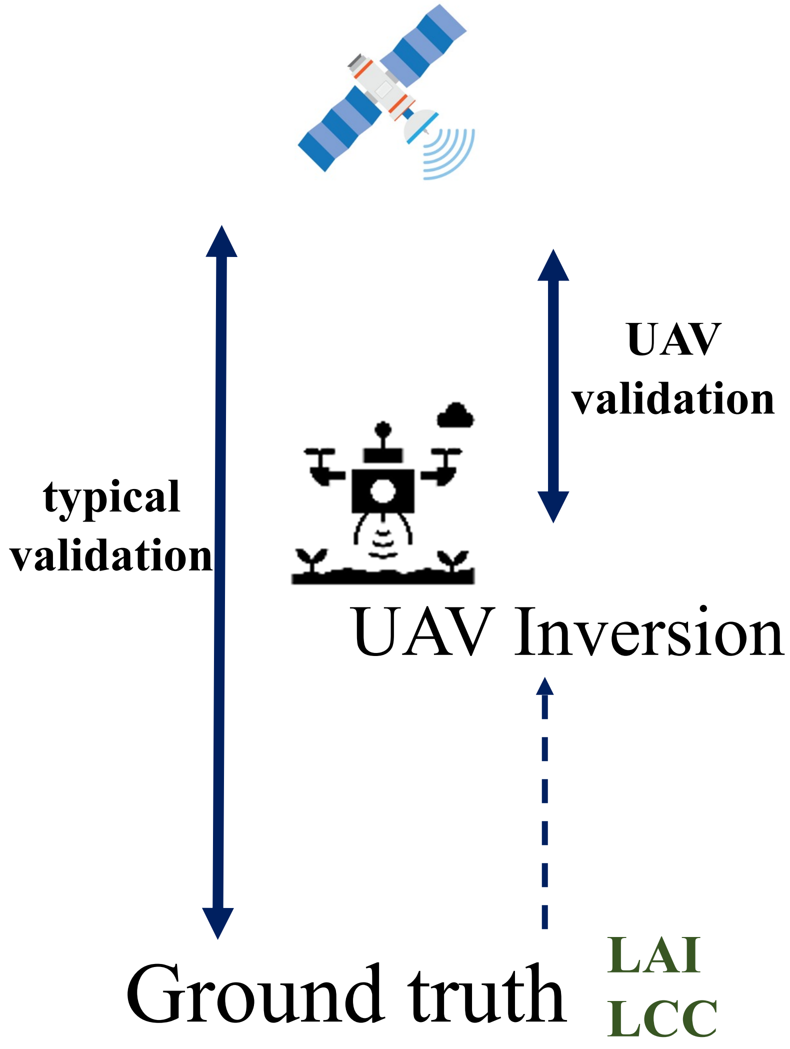

Project team


Dr Jadu Dash


Dr Yongjun Zhang


Dr Yan Gong


Dr Joanne Nightingale


Dr Gareth Roberts


Dr Booker Ogutu


Dr Yansheng Li


Hu Tang


Niall Origo


Rosalinda Morrone

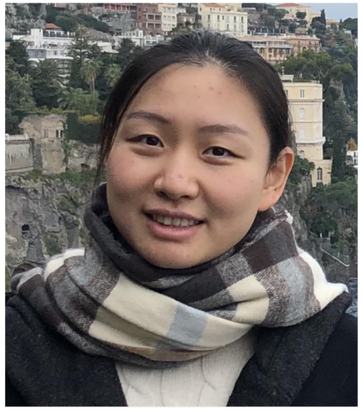
Xuerui Guo


Luke Brown


Harry Morris

University of Southampton

武漢大學 WUHAN UNIVERSITY

NPL National Physical Laboratory

Timeline

Protocols, procedures, training and calibration

Field Campaign in UK and China

Campaign data processing and delivery

Dissemination and outreach

Exchange and Sharing of Resources

Year 1

Year 2

Year 3

Year 4

Timeline

Initial field data collection

Further field data collection

timeline of key points

2021

2022

2023

2024

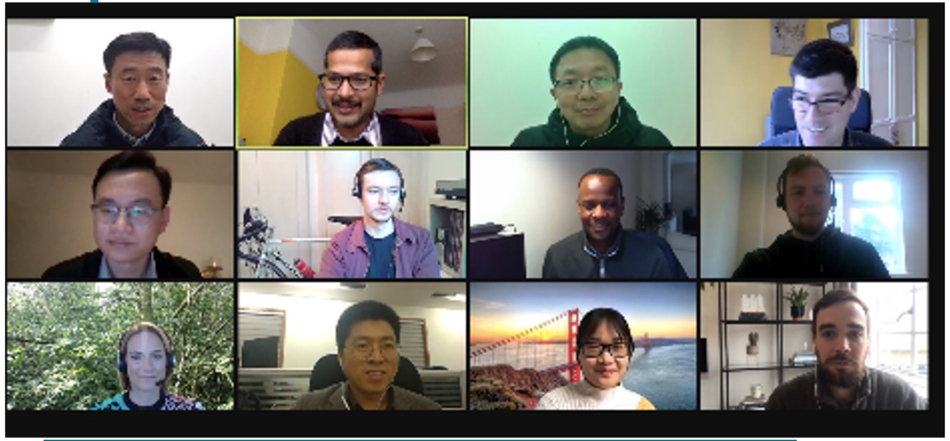

KO meeting Dec 2020

Application of FRM protocol, training and exchange visit

The in-situ data measurements and requirements

ESA Third Party Missions	No. Scenes
1. Sentinel 2 MSI	10

Chinese EO data	No. Scenes
1. Gaofen-6	**6**

Campaign	Period	Parameters and equipment	Contribution
Taizi Mountain, China (112°48′E-113°03′E, 30°48′N-31°02′N)	31-10-2020 01-11-2020 02-06-2021	LAI-2200C for LAI collection ASD spectrometer for Spectral data collection DJI Phantom 4 for UAV images collection	Wuhan University
Luojia Square, China (114°21′E-114°22′E, 30°32′N-30°33′N)	19-12-2020	ASD spectrometer for Spectral data collection DJI Phantom 4 for UAV images collection	Wuhan University
Wytham Woods, UK (51.769265N, 1.329185W)	19-07-2021	SPAD for LCC collection Digital hemispherical photography(DHP)	University of Southampton, National Physical Laboratory (NPL)

Field data collection campaigns

Taizi Mountain Hubei Province, China

- Deciduous broadleaf forest
  - (Oak and Maple)
- National Park
- Validation of SPOT 6 and GF 2 at site
- > 35 remote sensing papers at site

DJI Phantom 4

ASD spectrometer

Field data collection campaigns

Taizi Mountain Hubei Province, China

- Surface reflectance and drone images
    - Ground Hyperspectral measurements (350 – 2500 nm)
    - DJI Phantom 4 for drone image collection
    - In-suit data collection-LAI-2200C

ASD Fieldspec 4

DJI Phantom 4

LAI-2200C

Field data collection campaigns

Wytham Woods, Oxford, UK

- Deciduous broadleaf forest
  - (Oak, Ash, Beech, Hazel, Sycamore)
- Managed research forest with ~75 years of ecological monitoring
- Canopy walkway, Flux tower
- > 200 RS papers at site

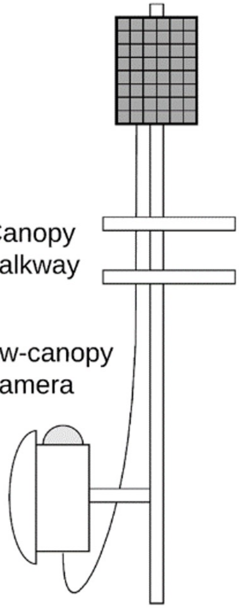

Field data collection campaigns

Wytham Woods, Oxford, UK

- leaf sampling and chlorophyll measure
- DHP measure
- CCC = LCC x LAI

Licor LAI-2200

Digital hemispherical photography

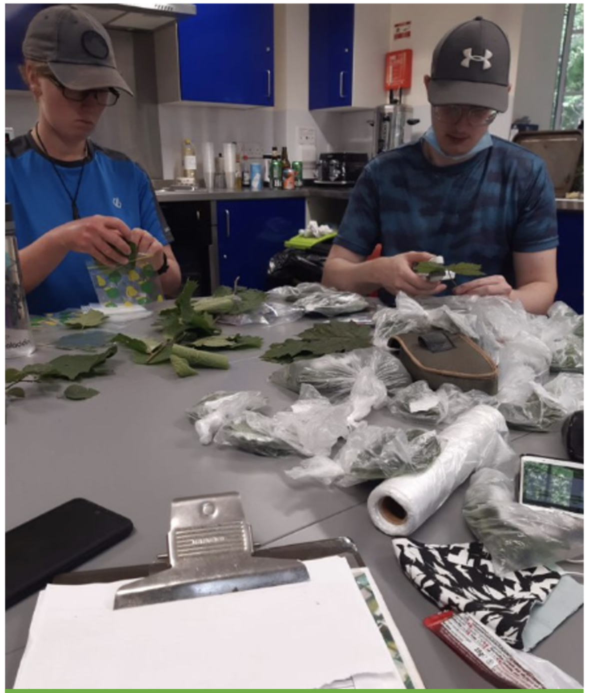

SPAD Chlorophyll meter

Field data collection campaigns

Wytham Woods, Oxford, UK

- Sampling Strategy
  - 20 – 30 ESUs sampled
  - Adapted from VALERI methodology
  - Understory and overstory sampled
- LAI
  - 13 points/ESU
- LCC
  - 3 leaves/point
  - 6 replicates/leaf

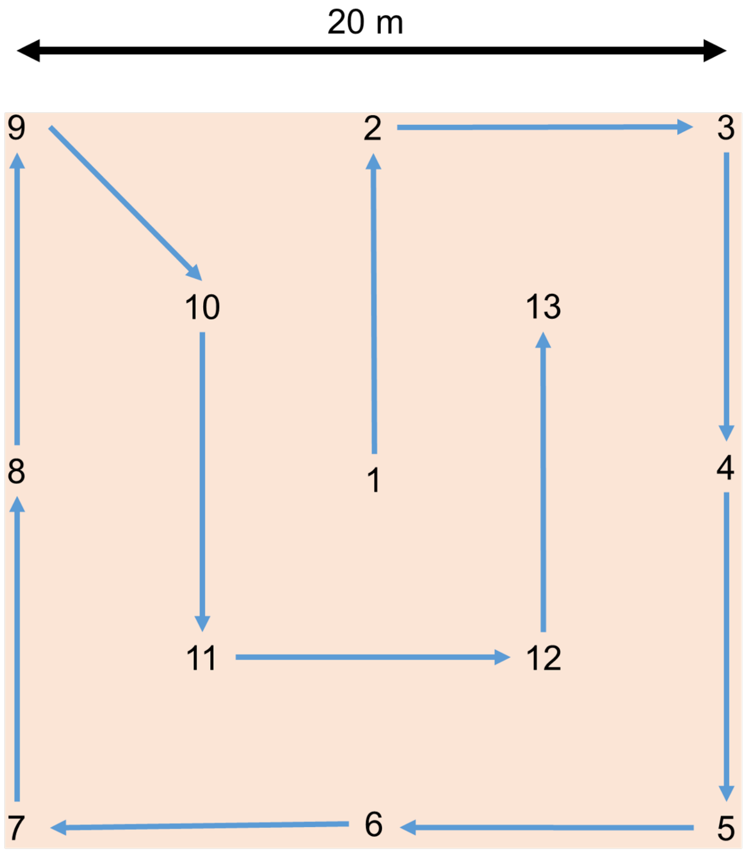

Method: Overview

Step 1	Step 2	Step 3	Step 4
Acquisition and processing of UAV imagery and in-suit biophysical measurements. Radiation calibration of UAV images	LAI Inversion from UAV imagery through Vegetation Indices (VIs) regression model. Sentinel-2 retrieved LAI product from ESA SNAP software.	VIs sensitivity test on a Radiative Transfer Model (RTM)-simulated dataset.	Sentinel-2 LAI product validated by the UAV based LAI product.

Method: Radiation calibration of UAV images

Radiometric Correction: Single image VS multiple images

The radiometric calibration methods suitable for a single image may become impractical for multiple UAV images.

During the flight of a UAV, each image may be influenced by:

- **different exposure times**
- **different incident angles,**
- **different illumination conditions**
- **different turbulence.**
- **……**

Method: Radiation calibration of UAV images

The multi-scale UAV image joint radiation correction method

UAV image pixels (DN)

Low-altitude image (40m)

Relative calibration

High-altitude image (450m)

Used as Reference image

Absolute calibration

Ground Measured Reflectance

The multi-scale UAV image joint radiation correction method

- **Histogram matching method**

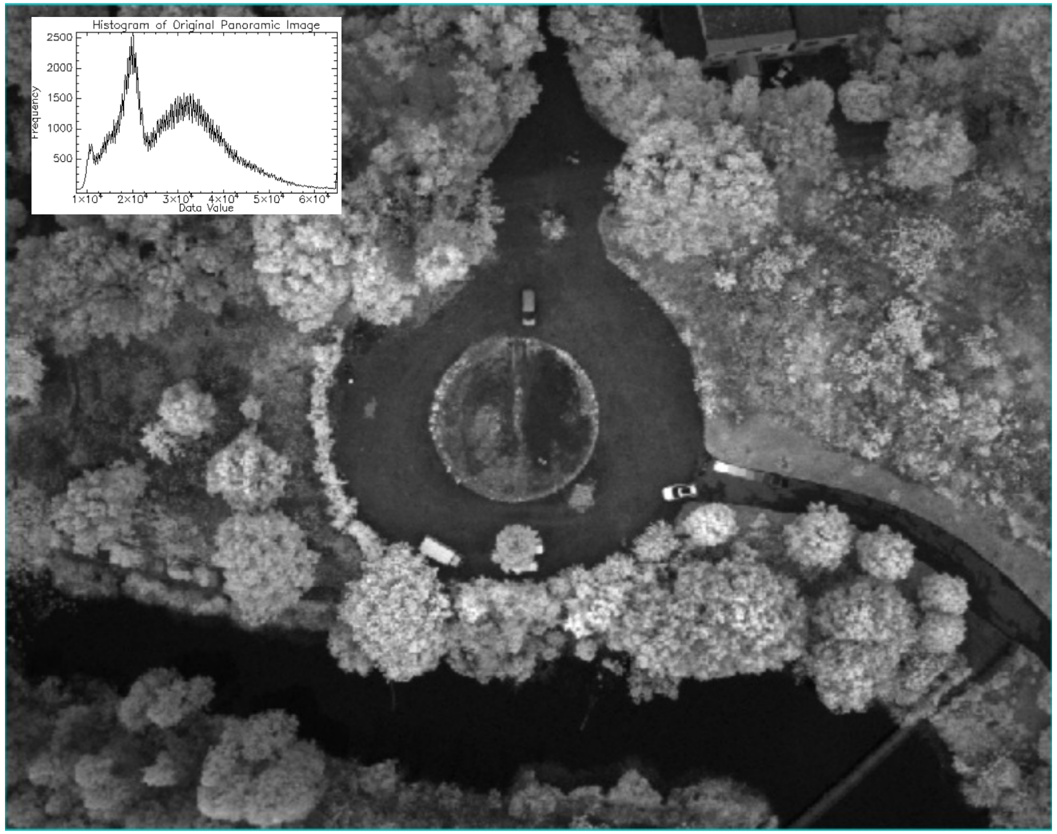

High-altitude image (450m)

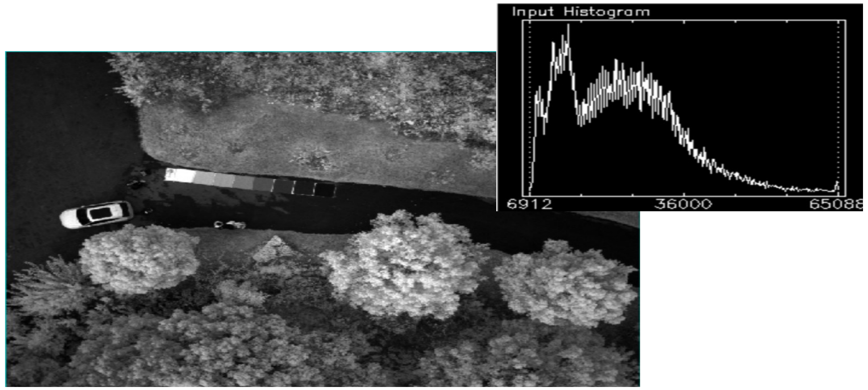

Before histogram matching

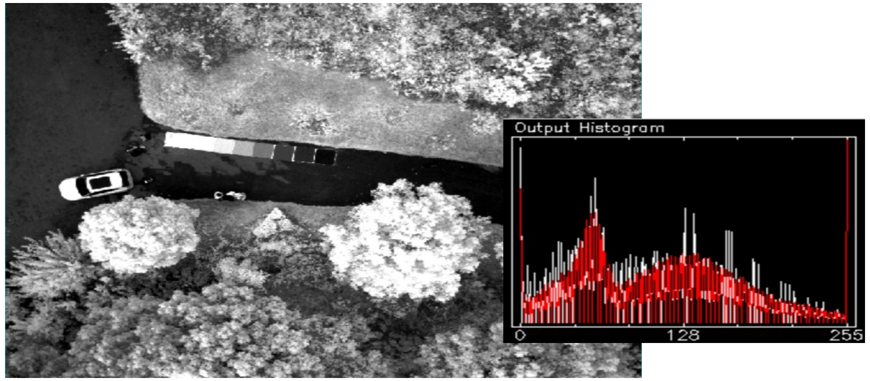

After histogram matching

Method: Radiation calibration of UAV images

The multi-scale UAV image joint radiation correction method

- Linear regression with SIFT operator
- Linear regression with multiple area

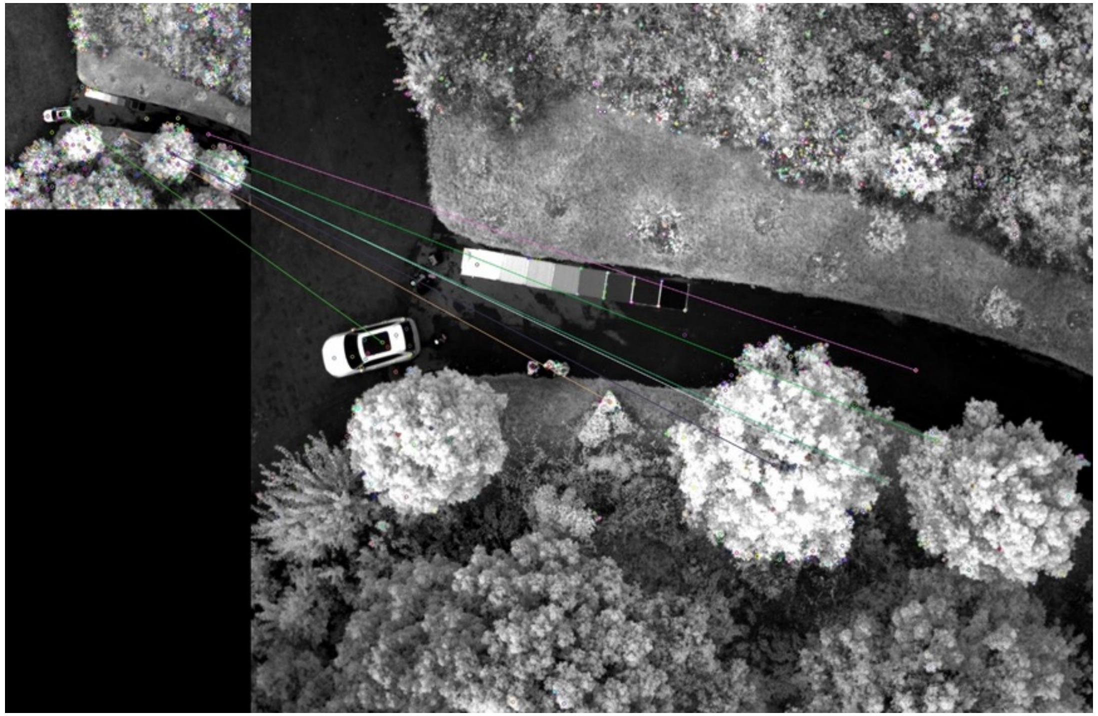

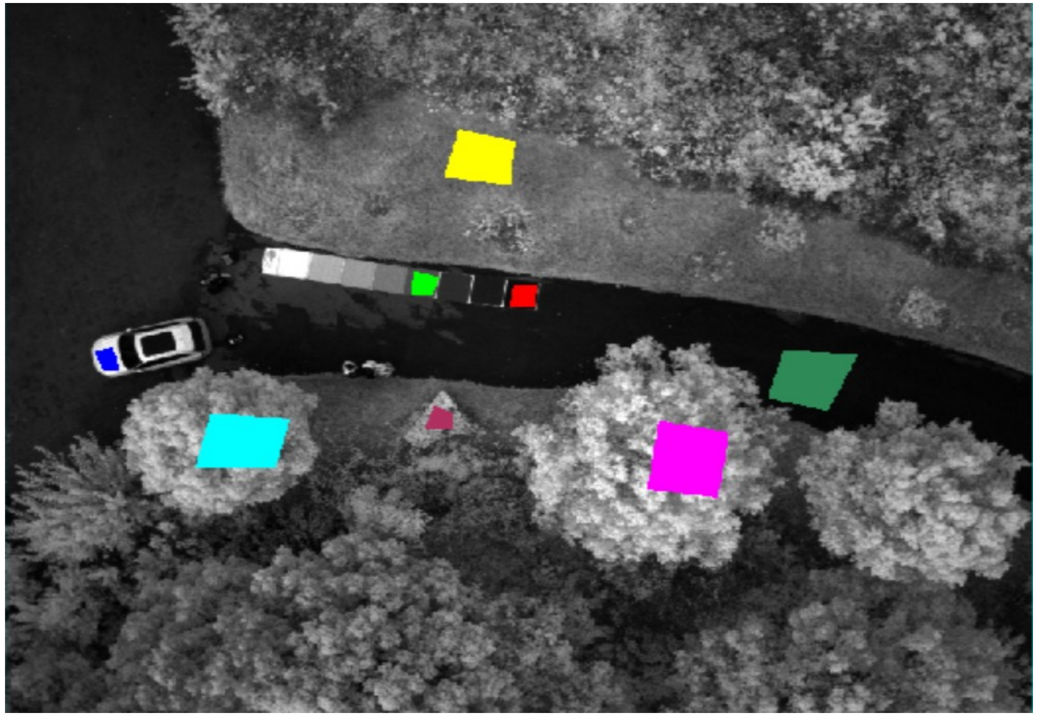

Taking High-altitude image as a reference, the relative radiometric correction is made for each image

A Radiometric Correction Method Based on Block Adjustment

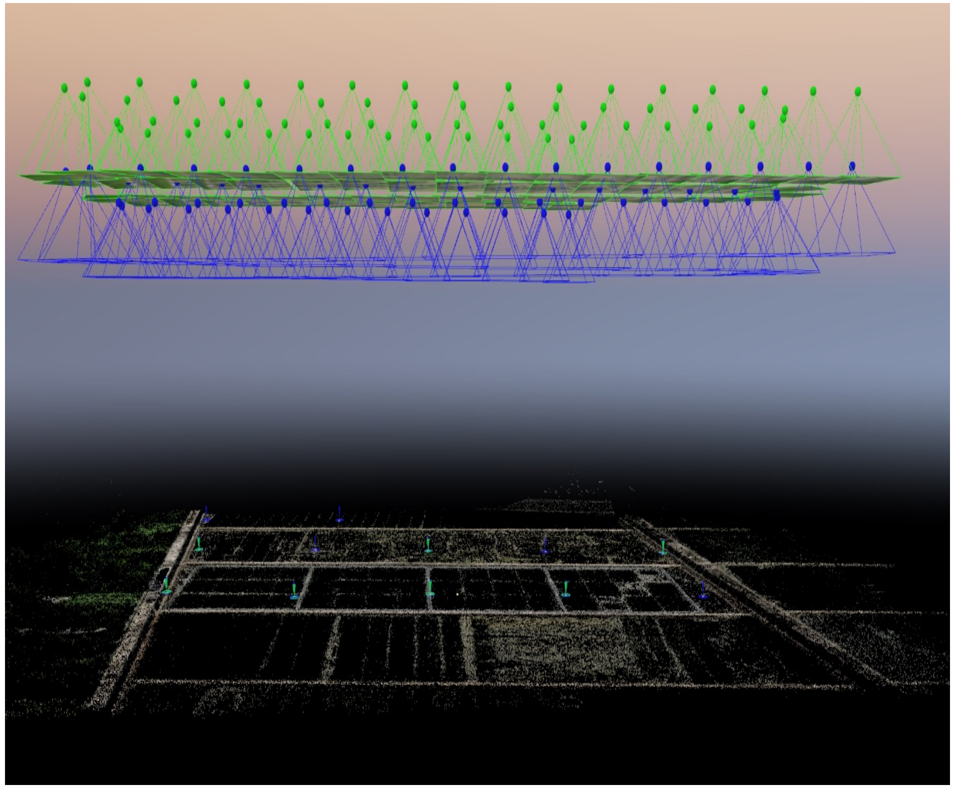

Geometric Correction Research: (photogrammetry)

- Using ground control points (**GCPs**) and tie points (**TPs**),block adjustment (**BA**) can effectively eliminate geometric errors.

Block Adjustment method used in Radiometric Correction?

- Radiometric calibration of multiple UAV images using only **a small number of calibration blankets**, thereby generating reflectance mosaics of the entire study area.

Method: Radiation calibration of UAV images

A Radiometric Correction Method Based on Block Adjustment

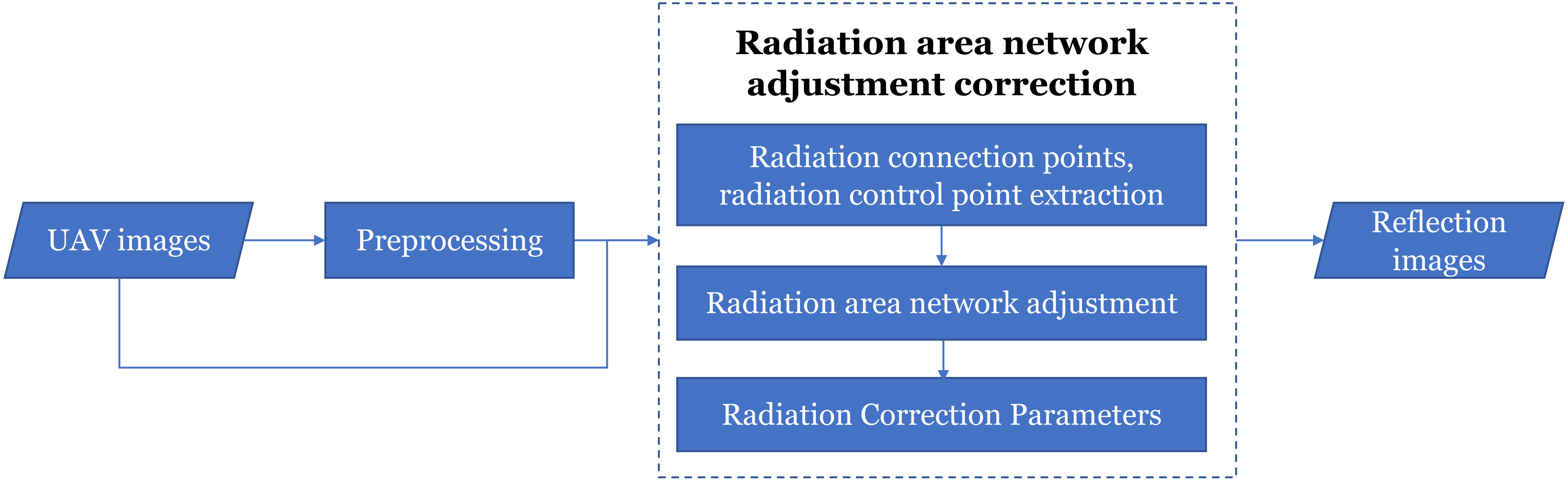

Method work flow

Method: Radiation calibration of UAV images

Radial Area Network Adjustment Algorithm

- Conversion relationship between DN value and reflectance
- Vignetting correction model
- Adjustment of light and dark differences between images
- Radiation area network adjustment
- Extraction of radial tie points
- Generation of stitched reflectance images

■ Radiometric Control Points (RCPs) : ground objects with known reflectance.

■ Radiometric Tie Points (RTPs): ground objects with radiometric observations.

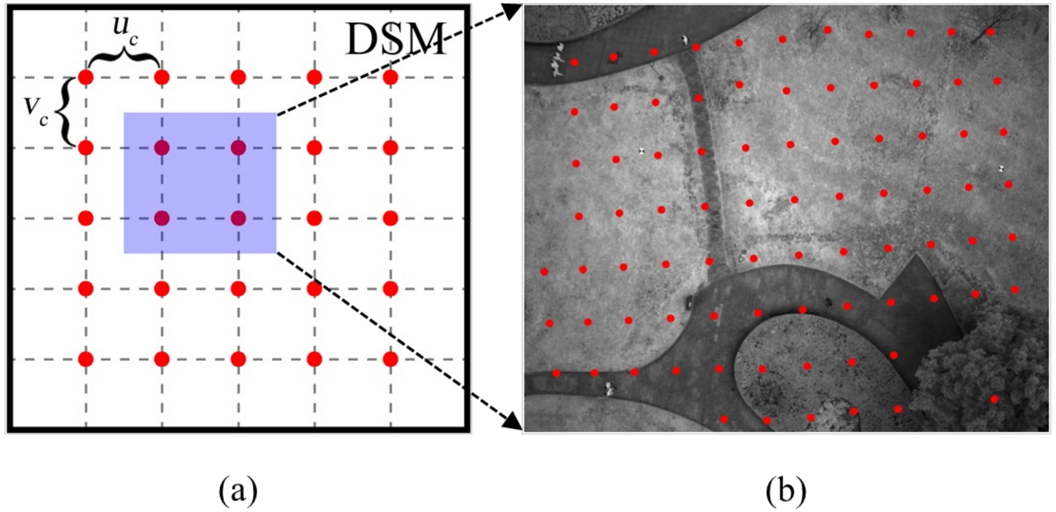

Fig. 2. Examples of (a) selection of RTPs from DSM. The parameters u_c and v_c are the intervals determined by the UAV image size and (b) distribution of RTPs on a UAV image. The red dots are the selected RTPs.

Method: Radiation calibration of UAV images

Radial Area Network Adjustment Algorithm: error equation

Reflectivity is an intrinsic property of ground objects. After radiation correction, the reflectivity of the same ground object should be the same.

Vignetting correction

$$V(u,v) = p_1(u-u_0)^2 + p_2(v-v_0)^2 + 1 = p_1u^2 + p_2v^2 + p_3u + p_4v + p_5$$

(u, v) Pixel coordinate

Radiation area network adjustment

$$V(u,v)DN_{ij} = a_i b \rho_{RTP,j}^{a} + b_i$$

$$V(u,v)DN_{ij} = a_i(a\rho_{RTP,j} + b) + b_i$$

DN_{ij} DN value of radiation connection point j on image i

$\rho_{RTP,j}$ Reflectivity of radiation connection point j

a,b Absolute correction parameters

a_i, b_i Relative correction parameters

Radial Area Network Adjustment Algorithm: error equation

Radiation area network adjustment

weight

$$v_{ij} = a_i(a\rho_{RTP,j} + b) + b_i - V(u,v)DN_{ij} \quad w_{ij}$$

Using Taylor Formula to linearize the error equation as follows:

$$v_{ij} = v_{ij}^0 + \frac{\partial v_{ij}}{\partial a}\Delta a + \frac{\partial v_{ij}}{\partial b}\Delta b + \frac{\partial v_{ij}}{\partial a_i}\Delta a_i + \frac{\partial v_{ij}}{\partial b_i}\Delta b_i + \frac{\partial v_{ij}}{\partial p_1}\Delta p_1 + \frac{\partial v_{ij}}{\partial p_2}\Delta p_2 + \frac{\partial v_{ij}}{\partial p_3}\Delta p_3 + \frac{\partial v_{ij}}{\partial p_4}\Delta p_4 + \frac{\partial v_{ij}}{\partial p_5}\Delta p_5 + \frac{\partial v_{ij}}{\partial \rho_{RTP,j}}\Delta \rho_{RTP,j}$$

Least squares adjustment, iterative operation

$$\boldsymbol{V} = \boldsymbol{Ax} - \boldsymbol{L}, \quad \boldsymbol{W}$$

$$\boldsymbol{x} = (\boldsymbol{A}^T\boldsymbol{WA})^{-1}\boldsymbol{A}^T\boldsymbol{WL}$$

The weight of radiometric tie points

The purity of RTP j in image i

$$p_{ij} = \sigma_{ij} / avg_{ij}$$

The weight of RTP j

$$w_{ij}^{1} = \exp(-3p_{ij}),$$

$$w_{ij}^{2} = -\exp(-(\theta_{v,ij} - \theta_{s,i})^2 / (2\sigma_{v,i}^2)) + 1.005,$$

$$\sigma_{v,i} = \sqrt{\frac{1}{n}\sum_{j}(\theta_{v,ij} - \theta_{s,i})^2}.$$

The final weight

$$w_{ij} = w_{ij}^{1} \cdot w_{ij}^{2}.$$

σ_{ij} : the standard deviation

avg_{ij} : the average of the DN values

$\theta_{s,I}$: the solar zenith

$\theta_{v,ij}$: the view zenith angle of the RTP j in image i

Reduce the influence of BRDF

(source: Peng W, et al. ,2023)

Parametric regression through Vegetation indices(VIs)

Formulas of the four VIs and the evaluation metrics for LAI-VI relationship modelling.

$$NDVI = \frac{\rho_{NIR} - \rho_{Red}}{\rho_{NIR} + \rho_{Red}}$$

$$SAVI = \frac{\rho_{NIR} - \rho_{Red}}{\rho_{NIR} + \rho_{Red} + 0.5} \times 1.5$$

$$ARVI = \frac{\rho_{NIR} - (2\rho_{Red} - \rho_{Blue})}{\rho_{NIR} + (2\rho_{Red} - \rho_{Blue})}$$

$$EVI = \frac{\rho_{NIR} - \rho_{Red}}{\rho_{NIR} + 6\rho_{Red} - 7.5\rho_{Blue} + 1} \times 2.5$$

$$R^2 = 1 - \frac{\sum_{i=1}^{n}(y_i - \hat{y}_i)^2}{\sum_{i=1}^{n}(\hat{y}_i - \bar{y})^2}$$

$$RMSE = \sqrt{\frac{\sum_{i=1}^{n}(y_i - \hat{y}_i)^2}{n - p}}$$

$$MAE = \sum_{i=1}^{n} \left| \frac{y_i - \hat{y}_i}{n} \right|$$

$$ME = \frac{1}{n} \sum_{i=1}^{n} \left(\frac{y_i - \hat{y}_i}{y_i} \right) \times 100$$

Sentinel LAI map inverted by PROSAIL model

- Sentinel-2 images preprocessing ⟶ Sentinel-2 reflectance images
- PROSPECT + SAIL model ⟶ The relationship between canopy reflectance and LAI
- ANN model ⟶ LAI inversion

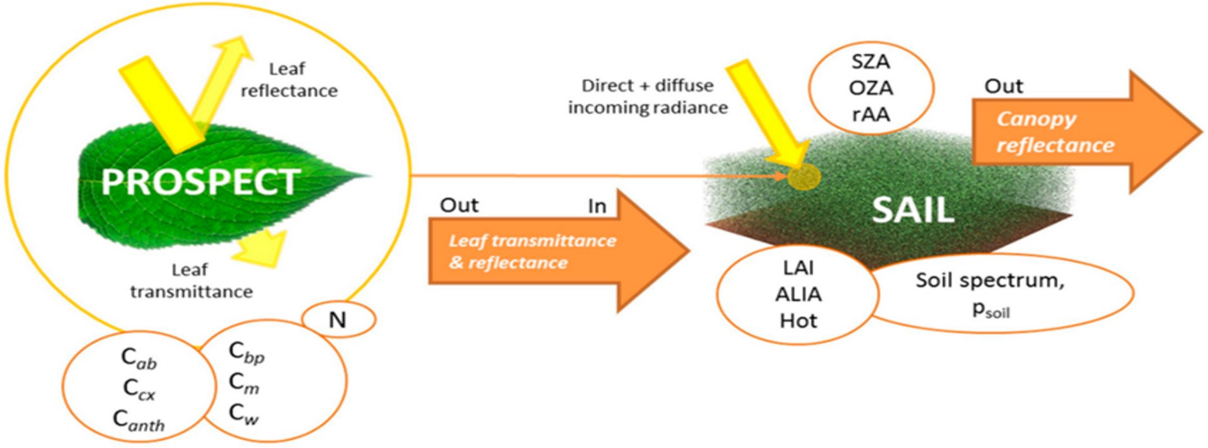

(source: Berger et al., 2018)

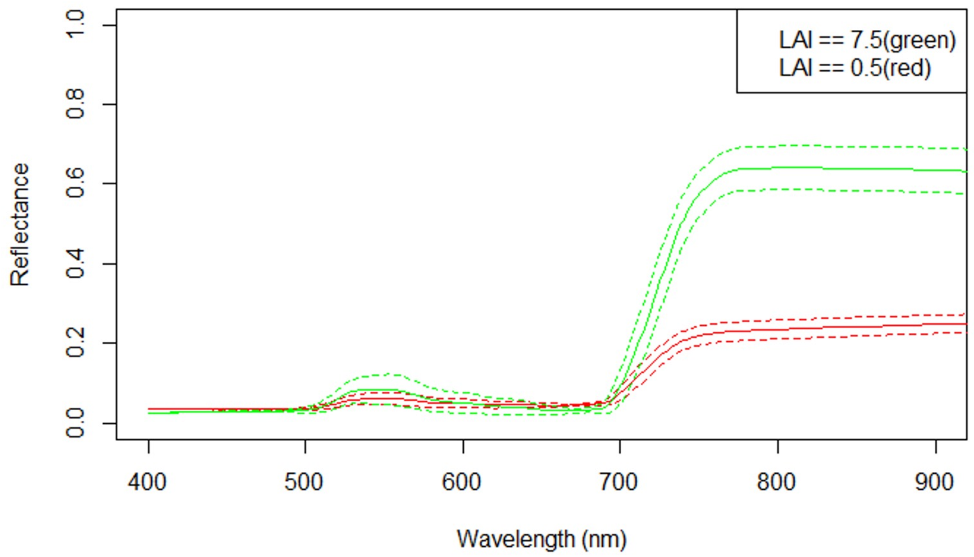

Method : LAI inversion from Gaofen-6

Gaofen-6 LAI map inverted by LUT

- Selecting VIs sensitive to LAI
  - Global sensitivity analysis of the PROSAIL model (NDVI, EVI, ARVI, SAVI)
- Generating LUTs
  - Reflectance-LUTs / VI-LUTs
- LAI retrieval based on LUTs
  - fRMSE → min

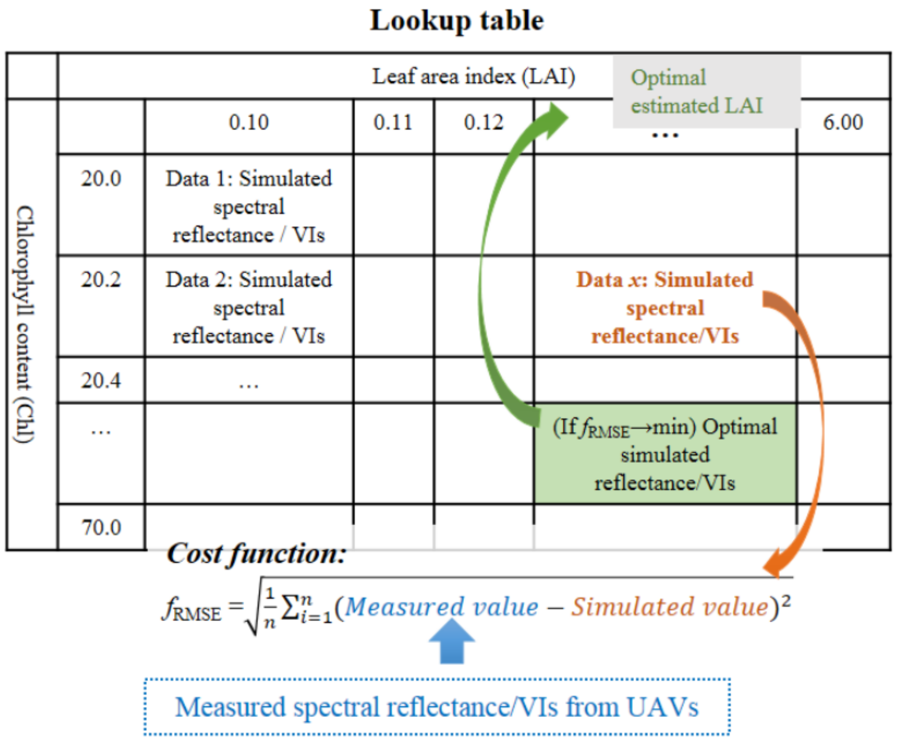

(source: Wanxue Zhu et al., 2019)

Satellite LAI validation using Ground-measures and UAV data

- For ground-measured data (P1)
    - 10 m *10 m Sentinel-2 and 16 m * 16 m Gaofen-6 pixel contained the ground measurements
- For UAV data (P2 & P3)
    - Resampled to Sentinel-2 andGaofen-6 spatial resolutions

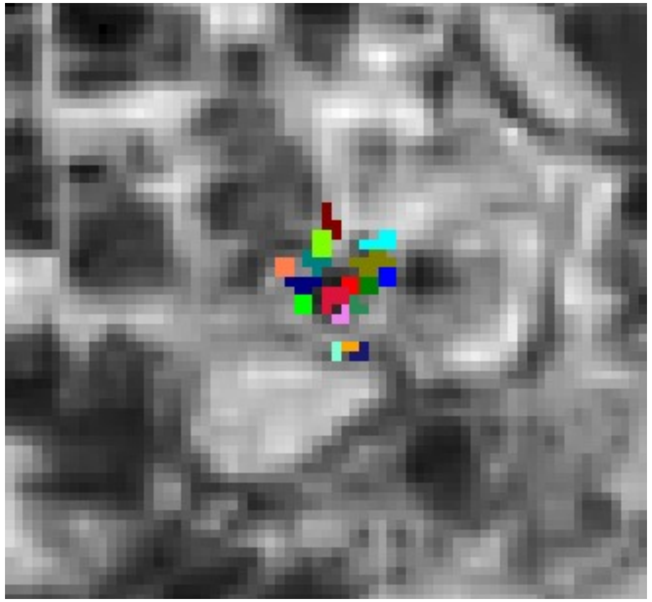

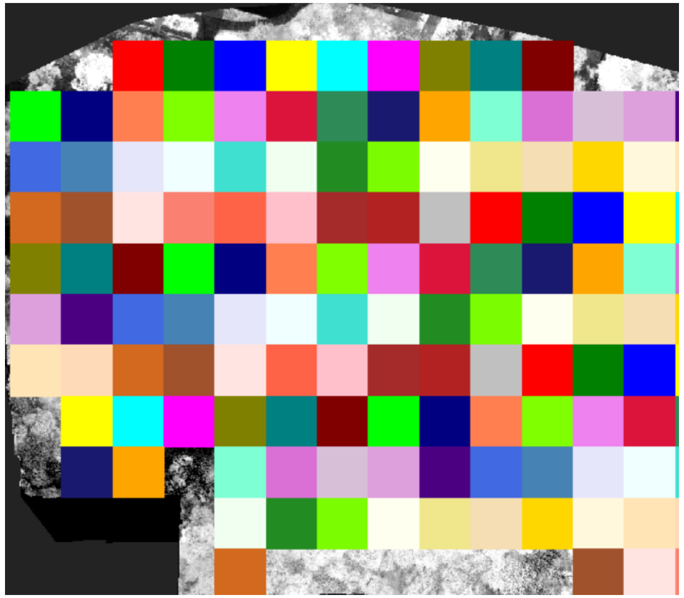

Result: Radiation calibration of UAV images

Visual radiation calibration results from four different methods

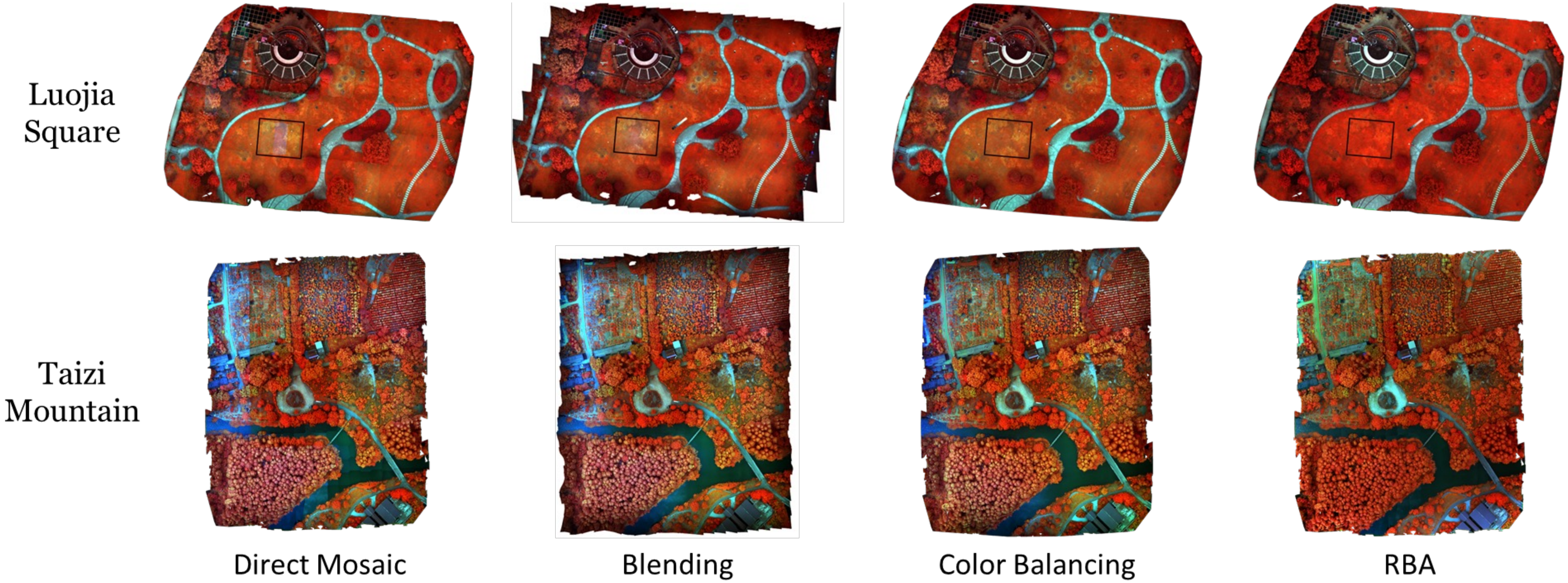

Results of Radiometric Calibration

Luojia Square

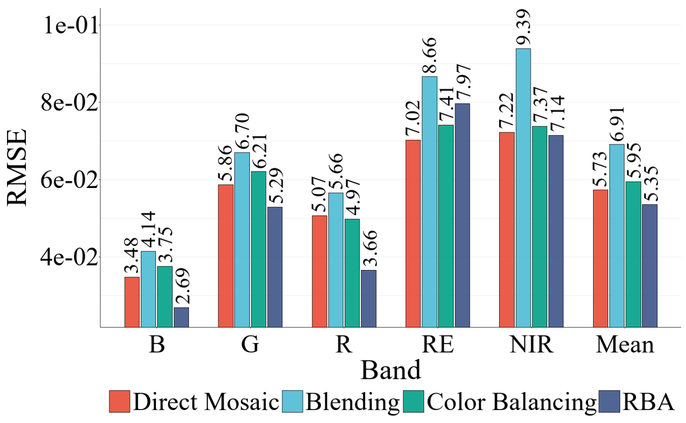

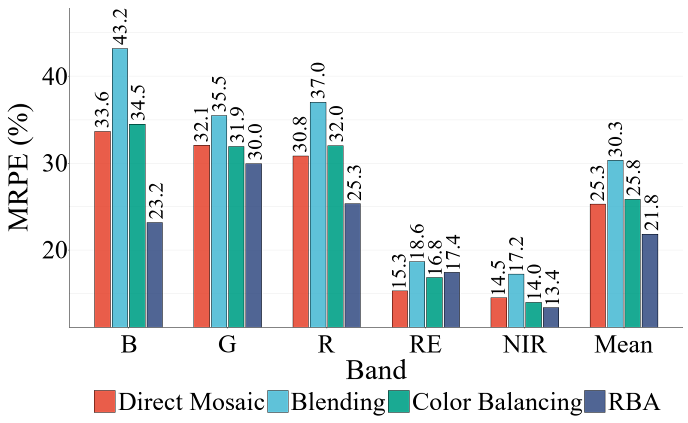

Taizi Mountain

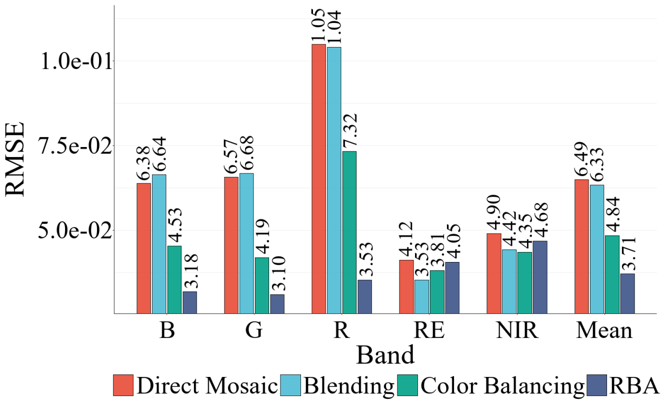

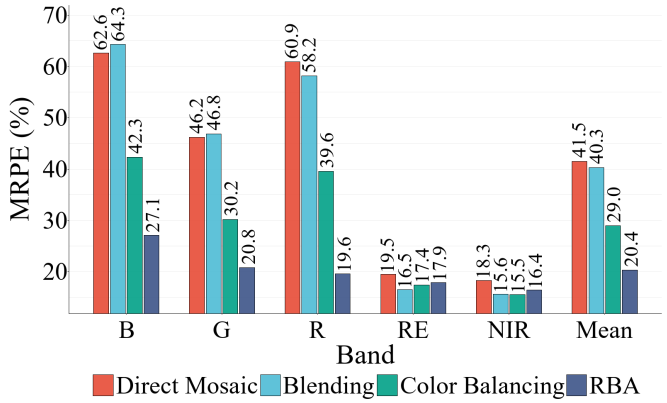

(source: Peng W, et al. ,2023)

Result: Radiation calibration of UAV images

Optimal number of RCPs

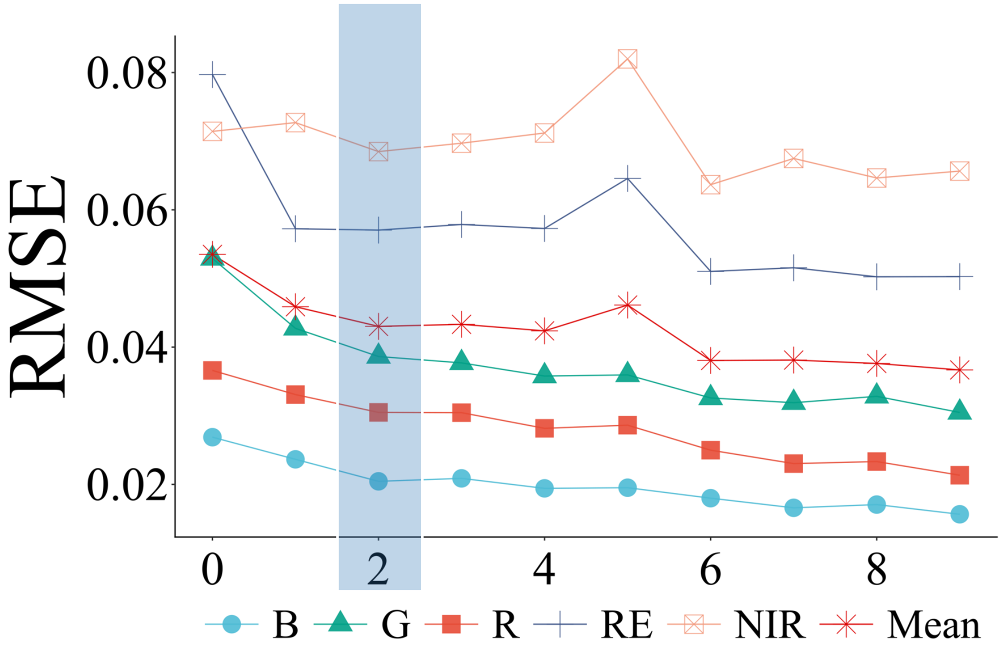

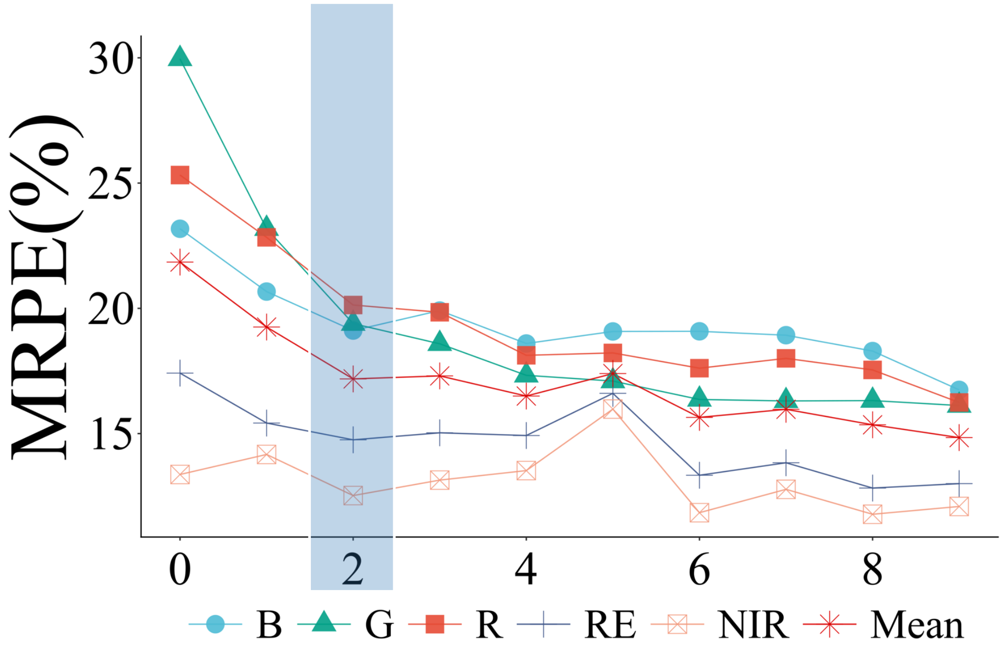

Adding certain number (2 point pairs in our study) of the radiation control points can effectively control the accumulation and propagation of errors and improve the accuracy of radiation correction.

Influences of Vignetting Correction on Radiometric Block Adjustment

- Vignetting correction can effectively improve radiometric calibration accuracy.
- RBA method integrates radiation area network adjustment and vignetting correction operations to avoid step-by-step calculations without affecting accuracy.

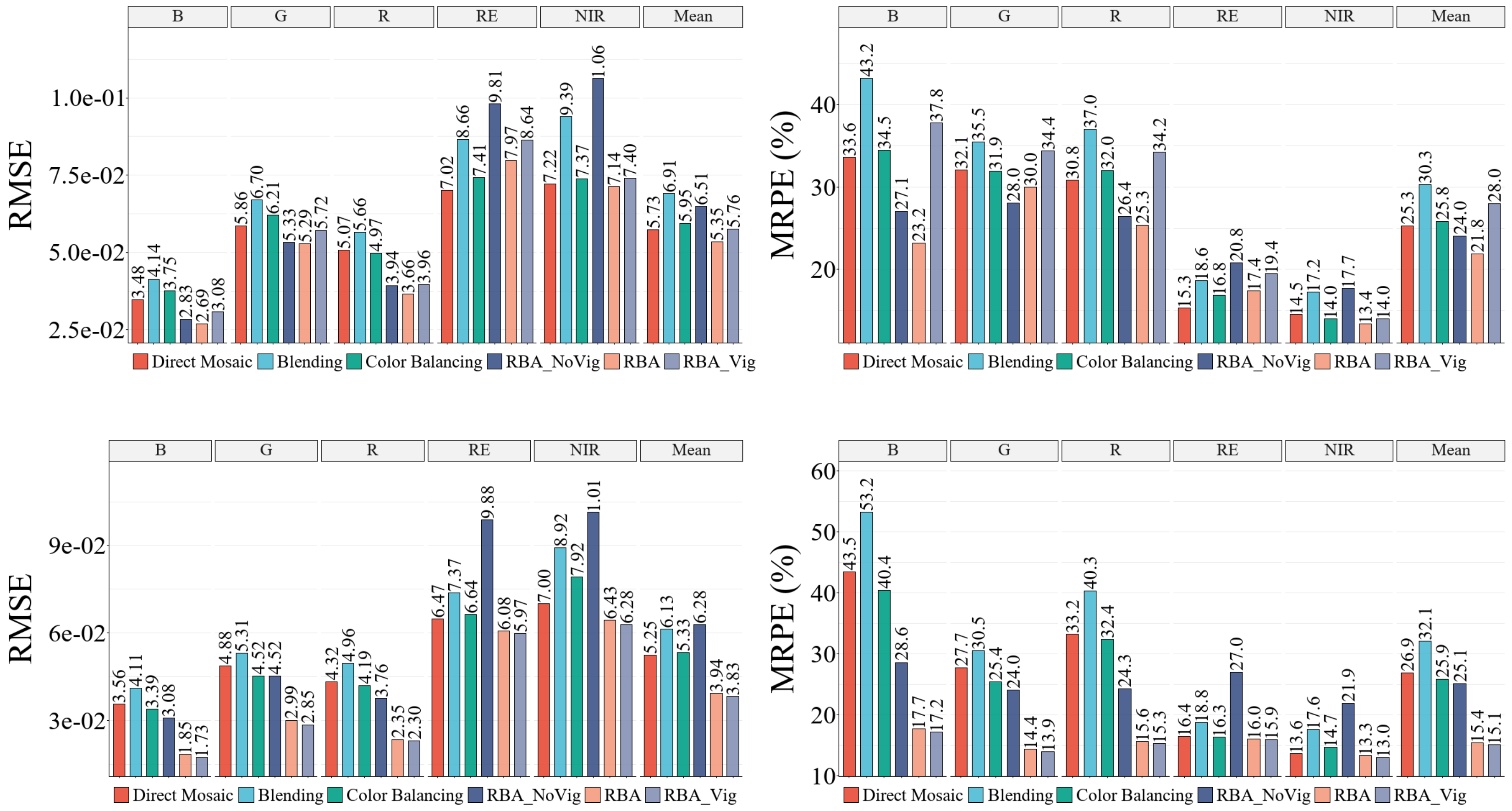

Result: Radiation calibration of UAV images

Uncertainty Analysis

- INFLUENCE FACTORS AND THEIR UNCERTAINTY (%)
- Among them, the weights, geometric mismatching, and noise had a relatively large impact on the radiometric correction accuracy, while the equation solution had little effect on the calibration results.

Luojia Square

Influence factor	B	G	R	RE	NIR
Weights	5.838	1.146	3.092	1.745	1.412
Geometric mismatching	2.926	1.045	2.491	0.713	1.143
Noise	4.721	1.518	2.255	1.504	1.288
Equation solution	0.001	0.001	0.000	0.001	0.000
Total uncertainty	8.058	2.170	4.566	2.412	2.227

Taizi Mountain

Influence factor	B	G	R	RE	NIR
Weights	3.102	1.723	1.399	2.146	0.955
Geometric mismatching	2.044	2.042	1.087	1.910	2.381
Noise	2.790	1.781	2.024	1.266	1.866
Equation solution	0.001	0.001	0.001	0.001	0.000
Total uncertainty	4.646	3.211	2.690	3.140	3.172

Result: LAI inversion from UAV imagery

UAV LAI maps inverted from UAV and Ground LAI

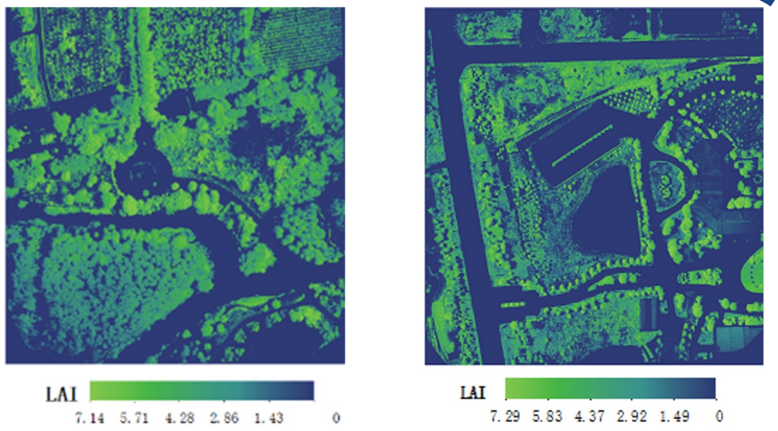

NDVI-LAI

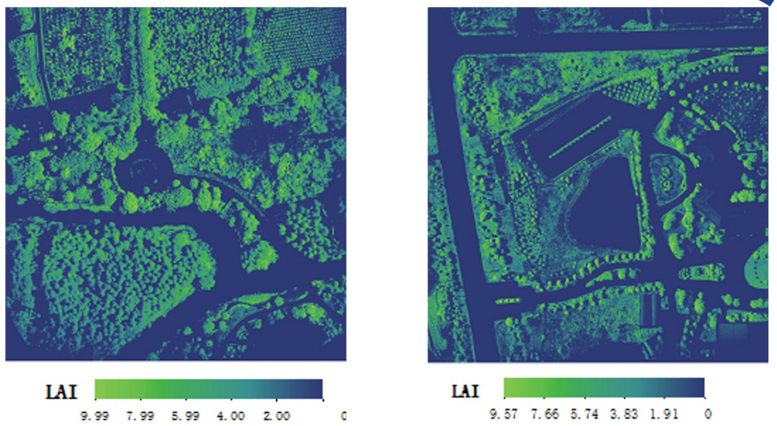

SAVI-LAI

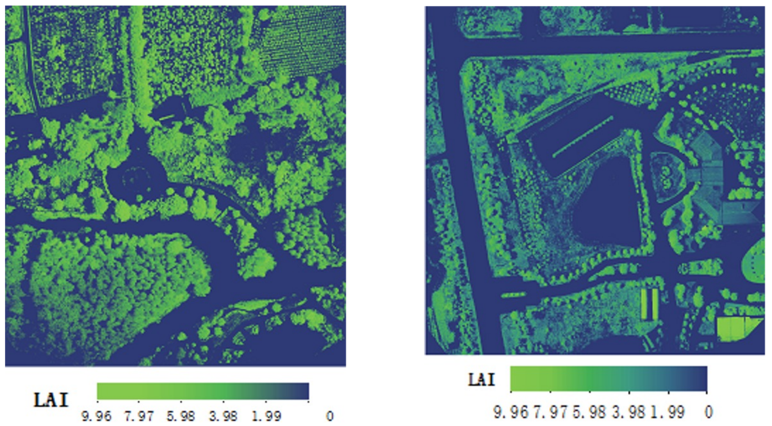

ARVI-LAI

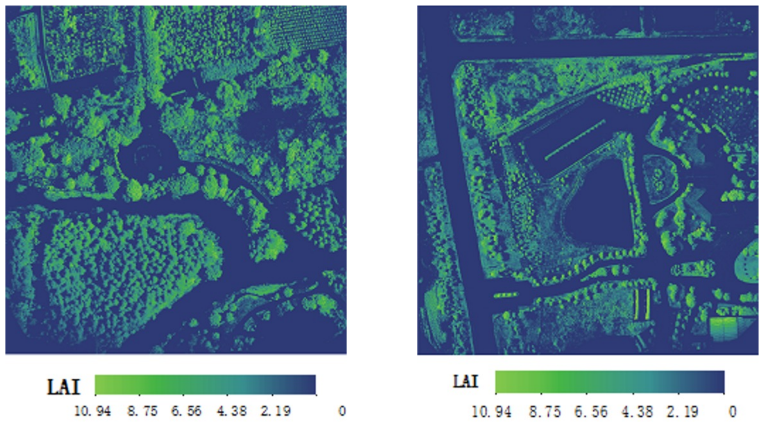

EVI-LAI

Result: LAI inversion from Sentinel-2 and Gaofen-6

- Sentinel-2 LAI map inversion from PROSAIL model

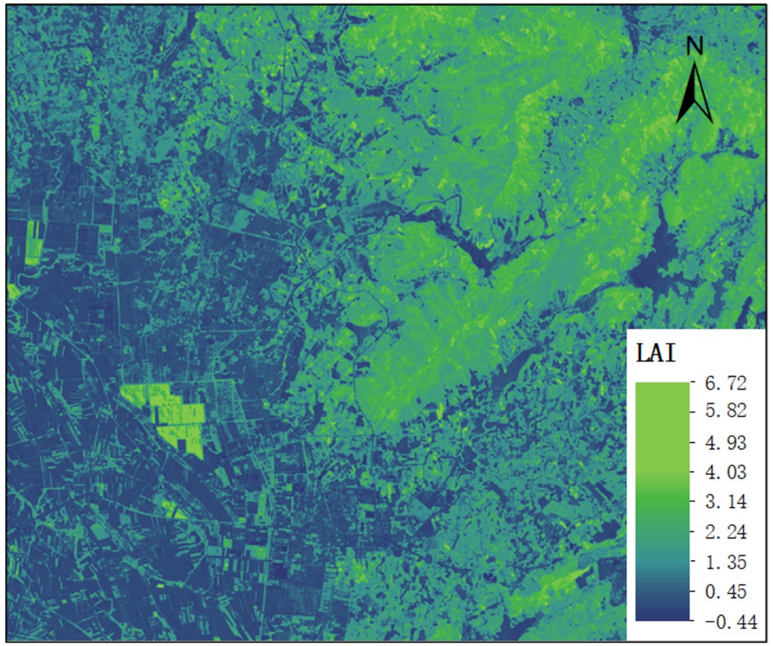

- Gaofen-6 LAI map inversion from LUT

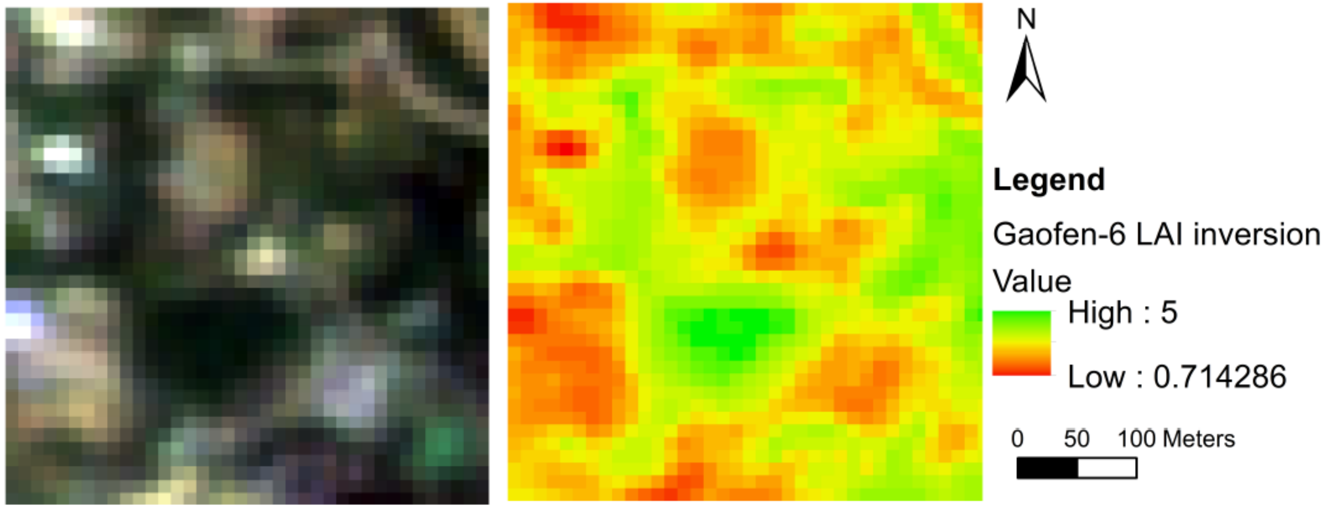

Result: Satellite LAI validation

Ground measurements vs. UAV-based LAI maps for validating satellite LAI retrievals

- Both the Sentinel-2 and Gaofen-6 LAI products perform moderately using UAV maps
- When we use UAV for validation, compared with ground validation methods
  - For Sentinel-2 LAI maps, lower MAE (≤ 0.5), ME (≤ 0.73) and RMSE (≤ 0.59) values were obtained
  - For Gaofen-6 LAI maps, the RMSE values were lower than 0.91 for all VI-based UAV LAI maps

Validation Method	Sentinel-2			Gaofen-6	
	MAE	ME	RMSE	MAE	RMSE
LAI samples based on ground-measured	0.80	0.85	1.02	1.08	1.58
UAV LAI maps generated based on NDVI	0.50	0.55	0.59	0.6.	0.77
UAV LAI maps generated based on SAVI	0.48	0.73	0.58	0.70	0.89
UAV LAI maps generated based on ARVI	0.48	0.55	0.58	0.59	0.76
UAV LAI maps generated based on EVI	0.47	0.67	0.56	0.71	0.91

Conclusion & Future Plan

Conclusion

- The RBA method can effectively improve the accuracy of UAV image radiation calibration.
- Gaofen-6 imagery showed great potential in estimating LAI through a LUT way by coupling the band wavelength with the radiative transfer model PROSPECT
- Compared the LAI validation results based on direct ground measurements and the estimated UAV-LAI map, significant improvement results were found with the high-resolution UAV-LAI map, RMSE reduced for Sentinel-2 and Gaofen-6 imagery.

Future plan

- The potential of Gaofen-6 to invert LAI using PROSAIL model
- The further acquisition of multispectral and even hyperspectral data from the UAV platform is expected.
- More fieldwork and communication in person from the collaborate institutes are planned.

European Young scientists contributions in Dragon 5

Name	Institution	Poster title	Contribution including period of research
Xuerui Guo	University of Southampton	Vegetation Index Sensitivity Test Based on PROSPECT+SAIL Model – a Preliminary Test Under the UAV4VAL Project	
Harry Morris	University of Southampton	Using A Wireless Quantum Sensor Network To Monitor The Temporal Dynamics Of Vegetation Biophysical Parameters In A Mediterranean Vineyard	

Chinese Young scientists contributions in Dragon 5

Name	Institution	Poster title	Contribution including period of research
Tang Hu	Wuhan University	Exploiting UAS for validating Sentinel-2 LAI map and inverting Gaofen-6 LAI map	data collection and data processing model establishment, data analysis, paper writing
Yang Kaili	Wuhan University	Remote estimation of leaf area index (LAI) with unmanned aerial vehicle (UAV) imaging for different rice cultivars throughout the entire growing season	data collection and data processing paper writing
Zhou Cong	Wuhan University	Combining spectral and wavelet texture features for unmanned aerial vehicles remote estimation of rice leaf area index	data collection and data processing paper writing
Yuan Ningge	Wuhan University	UAV Remote Sensing Estimation of Rice Yield Based on Adaptive Spectral Endmembers and Bilinear Mixing Model	data collection and data processing paper writing
Peng Wanshan	Wuhan University	A radiometric block adjustment method for unmanned aerial vehicle images considering the image vignetting	data collection and data processing paper writing

The peer reviewed publications

[1] Gong Y, Yang K, Lin Z, et al. Remote estimation of leaf area index (LAI) with unmanned aerial vehicle (UAV) imaging for different rice cultivars throughout the entire growing season[J]. Plant Methods, 2021, 17(1): 1-16.

[2] Zhou C, Gong Y, Fang S, et al. Combining spectral and wavelet texture features for unmanned aerial vehicles remote estimation of rice leaf area index[J]. Frontiers in Plant Science, 2022, 13: 957870.

[3] Yuan N, Gong Y, Fang S, et al. UAV remote sensing estimation of rice yield based on adaptive spectral endmembers and bilinear mixing model[J]. Remote Sensing, 2021, 13(11): 2190.

[4] Peng W, Gong Y, Fang S, et al. A Radiometric Block Adjustment Method for Unmanned Aerial Vehicle Images Considering the Image Vignetting[J]. IEEE Transactions on Geoscience and Remote Sensing, 2023.